Chemical pathways and kinetic rates of the N(4S) + N2 → N3 solid phase reaction: could the N3 radical be a temperature sensor of nitrogen ices in dense molecular clouds?

Alejandro Mencos, Sendres Nourry, Lahouari Krim

Monthly Notices of the ROYAL ASTRONOMICAL SOCIETY

MNRAS **467,** 2150–2159 (2017) doi:10.1093/mnras/stx140

Chemical pathways and kinetic rates of the $N(^4S) + N_2 \rightarrow N_3$ solid phase reaction: could the N_3 radical be a temperature sensor of nitrogen ices in dense molecular clouds?

Alejandro Mencos,[1,2,3] Sendres Nourry[1,2] and Lahouari Krim[1,2]★

[1] *Sorbonne Universités, UPMC Univ. Paris 06, MONARIS, UMR 8233, Université Pierre et Marie Curie, 4 Place Jussieu, case courrier 49, F-75252 Paris Cedex 05, France*

[2] *CNRS, MONARIS, UMR 8233, Université Pierre et Marie Curie, 4 Place Jussieu, case courrier 49, F-75252 Paris Cedex 05, France*

[3] *Universidad de San Carlos de Guatemala. Ciudad Universitaria, Zona 12. Edificio T12. Departamento de Fisicoquúmica. Guatemala*

Accepted 2017 January 16. Received 2017 January 6; in original form 2016 December 1

ABSTRACT

Even though the N_3 radical has not yet been detected in the interstellar medium, its formation still remains a challenge. For a long time, bombardments of N_2 ices by energetic particles were the only way to from the azide radical as it was thought that ultraviolet (UV) photons were not strong enough to fragment the molecular nitrogen into N atoms. Consequently, it had been suggested that N_3 could be used as discriminator between ice radiolysis and ice photolysis until a very recent study that has shown that photodecomposition of molecular nitrogen by UV photons might also be a source of the azide radical. In contrast to all these nitrogen ice bombarding experiments, only two laboratory studies have investigated the N_3 formation where the reactants N and N_2 mixed in the gas phase were co-condensed at 12 K, and this raised a new question concerning whether $N + N_2 \rightarrow N_3$ took place in the solid phase or in the gas phase. The experimental results of these two studies are contradictory and the problem of the characterization of N_3 formation by co-condensing atomic N and molecular N_2 has persisted to the present day. In this paper, we give a clear answer to this question, by investigating the kinetic rates of the $N(^4S) + N_2 \rightarrow N_3$ reaction in the solid phase in the temperature range of 3–35 K. We find a rate constant of 7.7×10^{-23} s^{-1} $molecule^{-1}$ cm^3 for the azide radical formation in the solid phase and we provide new information on the N_3 infrared signature, which could be used to characterize the temperature and the structure of nitrogen ices.

Key words: astrochemistry – methods: laboratory: molecular – techniques: spectroscopic – ISM: molecules.

1 INTRODUCTION

N_3 has not been detected in the interstellar medium, but this does not imply its astronomical non-existence. However, the absence of the azide radical from the interstellar environment might be surprising as nitrogen atoms are actually available inside some dark molecular clouds (Maret, Bergin & Lada 2006) and, in many experimental studies involving atomic nitrogen that try to mimic the conditions of molecular clouds or the cold atmospheres of planets, N_3 is detected as a subproduct. From a laboratory simulation point of view, the N_3 azide radical has been the subject of numerous discussions during the last 60 yr. These debates began with its proper normal vibrational mode analysis in 1956, when Milligan, Brown & Pimentel (1956) erroneously assigned an infrared (IR) absorption signal at 2150 cm^{-1} to the ν_3 N–N asymmetric stretching of N_3. Many decades later, Tian, Facelli & Michl (1988) determined the right ν_3 attribution by measuring its IR signature around 1657 cm^{-1} using keV fast atom and ion bombardment of N_2 matrices at 20 K. From this study, many vibrational frequencies of N_3 isotopomers and N_3^- anions have been reported for the first time (Table 1).

Thereafter, many groups have supported the N_3 assignments by Tian et al., using similar experiments in which nitrogen solids have been bombarded by different sources of energy (Gerakines, Schutte & Ehrenfreund 1996). It has even been suggested that N_3 could be used as a discriminator between ion-irradiated ices (ice radiolysis) and ices exposed to UV photons (ice photolysis); in the former case, N_3 is formed efficiently while it has never been observed in the latter case (Hudson & Moore 2002). Nevertheless, a very recent study carried out by Wu et al. (2012) has shown that UV photolysis of solid nitrogen can also lead to the formation of the N_3 radical. In contrast to all those bombarding solid nitrogen laboratory

★ E-mail: lahouari.krim@upmc.fr

Table 1. ν_2, ν_3 and $\nu_1 + \nu_3$ vibrational frequencies (cm^{-1}) of N_3 and N_3^- isotopomers (a '–' denotes not measured).

	ν_2	ν_3	$\nu_1 + \nu_3$
$^{14}N^{14}N^{14}N$	472.7	1657.5	2944.9
$^{14}N^{14}N^{15}N$	–	1649.3	2917.1
$^{15}N^{14}N^{15}N$	–	1639.7	2890.0
$^{14}N^{15}N^{14}N$	–	1621.4	2907.2
$^{14}N^{15}N^{15}N$	–	1612.7	2878.4
$^{15}N^{15}N^{15}N$	457.1	1603.2	2848.5
$^{14}N^{14}N^{14}N^-$	–	2003.5	–
$^{14}N^{14}N^{15}N^-$	–	1993.0	–
$^{15}N^{14}N^{15}N^-$	–	1982.1	–
$^{14}N^{15}N^{14}N^-$	–	1959.9	–
$^{14}N^{15}N^{15}N^-$	–	1949.0	–
$^{15}N^{15}N^{15}N^-$	–	1937.7	–

experiments, Khabasheku et al. (1997) and Amicangelo et al. (2007) studied N_3 formation where the reactants N and N_2 are mixed in the gas phase and then co-condensed at 12 K. From these two specific studies, one question has been raised concerning whether the N_3 radical is formed in the gas phase either through the $N + N_2$ reaction and then trapped in the solid nitrogen or through the same reaction occurring on the surface of an N_2 solid. The problem is that the temperature-dependent depositions performed by Amicangelo et al. appear to be consistent with N_3 formation in the gas phase, while those given by Khabasheku et al. seem to conclude that $N + N_2$ takes place in the solid phase rather than in the gas phase. Thus, the issue of the characterization of N_3 formation by co-condensing atomic N and molecular N_2 has persisted until the present day.

In fact, Amicangelo et al. studied N_3 formation by condensing the output of a microwave plasma discharge of nitrogen gas on to a window maintained at 10 K. By performing temperature-dependent matrix depositions, Amicangelo et al. observed a decrease in the amount of N_3 when the deposition temperatures increased from 10 to 20 K, a behaviour more consistent with the formation of N_3 in the gas phase than in the solid phase. These results are not in agreement with the measurements performed by Khabasheku et al., who studied N_3 radical formation by co-condensing N_2 and energetic nitrogen atoms (20–120 eV) at 12 K. They showed an increase in the quantity of N_3 by increasing the deposition temperatures between 12 and 20 K, proving that N_3 would be formed through the $N + N_2$ reaction in the solid phase and not in the gas phase. To overcome such inconsistencies and to confirm that the $N + N_2$ reaction takes really place in the solid phase, Amicangelo et al. tried to adapt their results to the three-body kinetic model $N(^2D) + N_2 + N_2 \rightarrow N_3 + N_2$ to estimate the amount of N_3 formed in the gaseous phase. As an analogy with the O_3 formation in gaseous phase, the three-body collision $N(^2D) + N_2 + N_2 \rightarrow N_3 + N_2$ should follow the kinetic equation $k_3[N(^2D)][N_2]^2$ where the k_3 unknown rate constant has been suggested to range from k_{O3} to $100k_{O3}$. They then deduced that the lower and upper limits of the amount of N_3 formed in the gaseous phase should be 2.1×10^{14} and 1.5×10^{17} molecules, respectively. However, they calculated the integrated peak area of the ν_3 band of N_3 and, using the corresponding absorption coefficient given by Hudson & Moore (2002) ($\varepsilon = 7.2 \times 10^{-20}$ cm molecule^{-1}), they deduced the amount of N_3 trapped in solid nitrogen to be around 51×10^{17} molecules. From these two calculations, Amicangelo et al. suggested that the N_3 azide radical should be formed in the solid phase.

Because of these conflicting conclusions resulting from the thermal and kinetic analyses, we have carried out a new experimental study to characterize and control the $N + N_2$ reaction. In addition to the measurement of the rate constant of the azide radical formation in the solid phase, we provide new information on the N_3 IR signature, which could be used to characterize the temperature and the structure of nitrogen ices in space.

2 EXPERIMENTAL METHODS

Our experimental method has been described previously by Zins, Joshi & Krim (2011). The formation of the N/N_2 solid samples is carried out through condensation of atomic and molecular nitrogen as reactants on to a polished rhodiated copper mirror maintained at 3 or 10 K under a vacuum of 10^{-8} mbar. Molecular nitrogen is purchased from Messer, with a purity of 99.9995 per cent while N atoms are generated with a flux of about 10^{15} atoms cm^{-2} s^{-1} from a microwave discharge (SPECS, PCS-ECR) into N_2 gas with N_2 dissociation yields about 4 per cent. The samples are analysed using a Bruker 120 HR FT-IR spectrometer in the transmission-reflection mode between 4500 and 500 cm^{-1}, with a spectral resolution of 0.5 cm^{-1}. To characterize N_3 trapped in solid nitrogen, the following experiments have been performed.

(a) N/N_2 co-deposition at 10 K: the N/N_2 mixture stemming from the microwave discharge was deposited on a mirror maintained at 10 K. The sample was then left for 2 h at 10 K to reach equilibrium, while several IR spectra were recorded during this period to check the transformation of the system at deposition temperature. Afterwards, to control its evolution versus temperature, the sample was heated at 15, 20, 25, 30 and 35 K and, at each temperature step, an IR spectrum was recorded.

(b) N/N_2 co-deposition at 3 K: the same N/N_2 mixture was co-deposited on a mirror maintained at 3 K and, just as for the experiments carried out at 10 K, the sample was left for a few hours at 3 K to reach equilibrium. Then, the temperature of the sample was increased at different steps in the range of 3–35 K and, at each warming step, an IR spectrum of the sample was recorded to control the $N + N_2$ reaction.

(c) Monitoring in time the formation of N_3: the temperature of an N/N_2 solid sample formed at 3 K was increased and fixed at 15 K for more than 3 h to study the kinetics of the $N + N_2$ reaction without supplying additional energy to the system.

(d) UV-visible photo-irradiation of N_3: the N_3 radical trapped in solid nitrogen was irradiated with selected UV-visible photons to characterize its photodecomposition at different wavelengths.

3 RESULTS

3.1 N/N_2 co-deposition at 10 K

In several previous studies, the N_3 radical trapped in solid N_2 has been characterized by two IR signals at 1652 and 1657 cm^{-1} assigned to the ν_3 N–N asymmetric stretching mode, due to two different trapping sites in the nitrogen matrix (Tian et al. 1988; Khabasheku et al. 1997; Hudson & Moore 2002; Amicangelo et al. 2007; Jamieson & Kaiser 2007; Wu et al. 2012). However, from these studies, we can see that those two signals are directly linked to the method of generating N_3 radicals and also to the deposition temperature of the samples. The signal at 1657 cm^{-1} is supported when N_3 is formed using photon irradiation or energetic particle bombardments regardless of deposition temperatures (Tian et al.

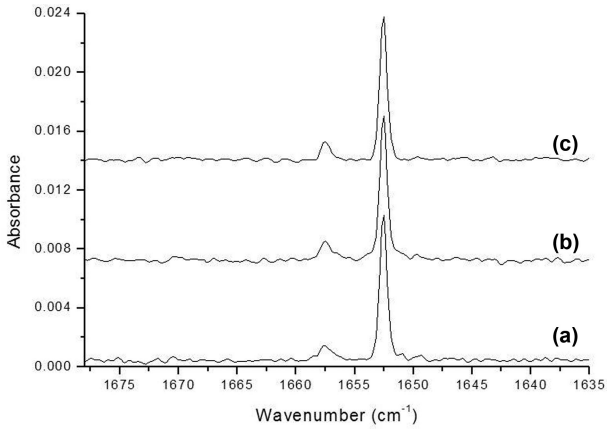

Figure 1. (a) Co-deposition of the N/N_2 mixture on a surface at 10 K and subsequent evolution of the solid sample kept at 10 K for (b) 1 h and (c) 2 h.

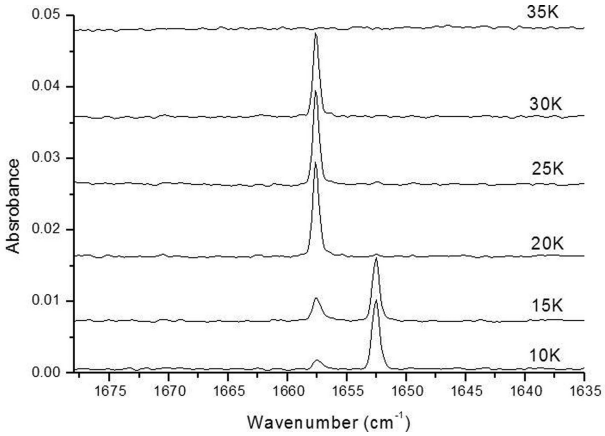

Figure 2. Co-deposition of the N/N_2 mixture at 10 K and successive sample heating between 10 and 35 K.

1988; Khabasheku et al. 1997; Hudson & Moore 2002; Jamieson & Kaiser 2007; Wu et al. 2012). When N_3 is produced by co-condensing non-energetic N atoms and molecular N_2, the signal at 1652 cm^{-1} is favoured when the deposition temperature is lower than 15 K, while at higher temperatures it degrades to favour that at 1657 cm^{-1} (Amicangelo et al. 2007).

Fig. 1 shows the spectrum, resulting from a co-deposition of N atoms and molecular N_2 on a mirror maintained at 10 K, which is similar to that presented by Amicangelo et al. Two signals at 1652 and 1657 cm^{-1} have been detected, corresponding to the two different trapping sites in the nitrogen matrix, labelled α and β, respectively, in the rest of this paper.

As shown in Fig. 1(a), the co-deposition of the N/N_2 mixture at 10 K leads to the formation of N_3 trapped mainly in site α, favoured at deposition temperatures lower than 15 K. The sample was then left for 2 h at 10 K to reach equilibrium. Figs 1(b) and (c) show the evolution of the two signals at 1652 and 1657 cm^{-1} characteristic of N_3 in solid nitrogen. After 1 h, we notice a tiny increase of the signal at 1657 cm^{-1} while that at 1652 cm^{-1} is almost constant. We reach equilibrium after 2 h as no evolution has been noticed in the recorded spectra. We have attributed the slight increase of the signal at 1657 cm^{-1} to the formation of N_3 due to the remaining atomic nitrogen in the sample. With these first results, we show that even though N_3 is produced directly during the sample deposition at 10 K, an additional amount of N_3 could also be generated in solid nitrogen and trapped in site β once the N_2 ice is formed. However, this slight increase in the amount of N_3 in the solid phase at 10 K might be the result of either the lack of nitrogen atoms in the solid nitrogen or the low mobility of the reactants at temperatures as low as 10 K.

The sample was then heated at temperatures of 15, 20, 25, 30 and 35 K and, at each temperature step, an IR spectrum was recorded to control the N_3 formation in the solid phase. As shown in Fig. 2, when the temperature of the sample increases, the signal at 1652 cm^{-1} decreases progressively between 10 and 20 K and disappears completely at temperatures higher than 20 K. Correspondingly, the signal at 1657 cm^{-1} increases between 10 and 20 K, reaches a constant level between 20 and 25 K, starts to decrease at temperatures higher than 25 K, and finally totally disappears at 35 K.

Knowing that the integrated areas of the two peaks at 1652 and 1657 cm^{-1} correspond to the amount of N_3 trapped in the two trapping sites α and β in solid nitrogen, respectively, and that their sum corresponds to the total amount of N_3 formed in our samples, it is worth noting that between 10 and 20 K, the decrease of the signal at 1652 cm^{-1} corresponds exactly to the increase of that at 1657 cm^{-1}, while the sum of the integrated peak areas remains constant during the increment of the temperature between 10 and 20 K. As the total amount of N_3 in our samples formed at 10 K remains constant while the sample is heated in the 10–20 K temperature range, we conclude that there is no evidence for N_3 formation in the solid phase but just a migration of the N_3 radical from the α to β trapping sites. Table 2 summarizes the evolution of the integrated peak areas at 1652 and 1657 cm^{-1} with the temperature to quantify the evolution of N_3 radicals trapped in the nitrogen matrix.

Table 2. Integrated peak areas S_α (cm^{-1}) and S_β (cm^{-1}) to quantify the amount of N_3 trapped in sites α and β and the total amount of N_3 formed between 10 and 20 K.

	N_3 in site α at 1652 cm^{-1}	N_3 in site β at 1657 cm^{-1}	Total N_3 in sites α and β at 1652 and 1657 cm^{-1}
T (K)	S_α (cm^{-1})	S_β (cm^{-1})	$S_\alpha + S_\beta$ (cm^{-1})
10	0.008	0.001	0.009
15	0.006	0.003	0.009
20	0	0.009	0.009

From Table 2, some thermodynamic properties such as ΔG, ΔH, ΔS and the equilibrium constant for the migration of N_3 from the trapping site α (1652 cm^{-1}) to site β (1657 cm^{-1}) can be deduced between 10 and 15 K. As the migration of the N_3 radicals occurs from the α to β trapping sites, the equilibrium constant can be written as

$$K = \frac{[N_3 \; in \; \beta \; site]}{[N_3 \; in \; \beta \; site]} = \frac{S_\beta}{S_\alpha} \quad (1)$$

where S_α and S_β are the integrated peak areas corresponding to the amount of N_3 trapped in sites α and β. From the equilibrium constant for a given temperature, the free energies of Gibbs ΔG, ΔH and ΔS can be deduced using

$$\Delta G = -RT \, Ln(K) = \Delta H - T\Delta S \quad (2)$$

$$Ln\left(\frac{K_{15}}{K_{10}}\right) = -\frac{\Delta H}{R}\left(\frac{1}{T_{15}} - \frac{1}{T_{10}}\right) \quad (3)$$

Table 3. ΔG, ΔH, ΔS and the equilibrium constant for the migration of N_3 from the trapping site α (at 1652 cm^{-1}) to site β (at 1657 cm^{-1}) between 10 and 15 K.

T (K)	K	ΔG (J mol^{-1})	ΔH (J mol^{-1})	ΔS (J mol^{-1})
10	0.125	172.9	345.8	17.3
15	0.5	86.4	345.8	25.9

Table 3 summarizes the thermodynamic properties for the migration of N_3 from site α to site β in the range of temperatures from 10 to 15 K.

A global conclusion from this first experimental study, carried out at 10 K, is that the whole amount of N_3 is formed during the deposition of the sample and there is no indication that N_3 is formed in the solid phase, as the heating of the sample to increase the motilities of the reactants shows just a migration of the N_3 radical from the α to β trapping sites.

As the efficiency of reactions occurring in the solid phase is a result of the reactant mobility, which should enhance at higher temperatures, generally proving that a given reaction occurs actually in the solid phase rather than in the gas phase, many experimental studies have to show an increase of the yield of the reaction products by increasing the deposition temperatures of the sample. This is what it has been achieved both by Khabasheku et al. and Amicangelo et al. to highlight the N_3 formation in the solid phase. However, as mentioned previously, the temperature-dependent depositions performed by Amicangelo et al. are consistent with the formation of the N_3 radical in the gas phase, while those given by Khabasheku et al. seem to conclude that $N + N_2$ takes place in the solid phase rather than in the gas phase. For these reasons, we prefer to study the influence of the decrease of the deposition temperature, from 10 to 3 K, on the yield of N_3, which should decrease considerably at 3 K if the $N + N_2$ reaction were to occur in the solid phase.

3.2 N/N_2 co-deposition at 3 K

The reactants N and N_2 have been co-deposited on a mirror maintained at 3 K and the result is illustrated in Fig. 3. At 3 K, only the signal at 1652 cm^{-1} corresponding to N_3 trapped in site α is detected with a very low intensity in comparison with results obtained with a deposition temperature of 10 K (Fig. 1). From calculations of the areas of the integrated peaks, we deduce that the total amount of N_3 formed at 3 K is 10 times lower than that formed at 10 K. Knowing that reactions occurring in ices depend highly on the mobility of the reactants, which enhances at higher temperatures (Khabasheku et al. 1997), we show that the $N + N_2$ reaction yield increases when the deposition temperature rises from 3 to 10 K. Thus, we conclude that N_3 formation occurs actually in the solid phase rather than in the gas phase, as otherwise we would have detected the same amount of N_3 at 3 and 10 K if the $N + N_2 \rightarrow N_3$ reaction had taken place in the gaseous phase followed by trapping N_3 in solid N_2. The comparison between Figs 3 and 1 also shows that at 3 K, N_3 is formed and trapped mainly in site α while at 10 K, 90 per cent of the total amount of N_3 is trapped in site α and 10 per cent in site β.

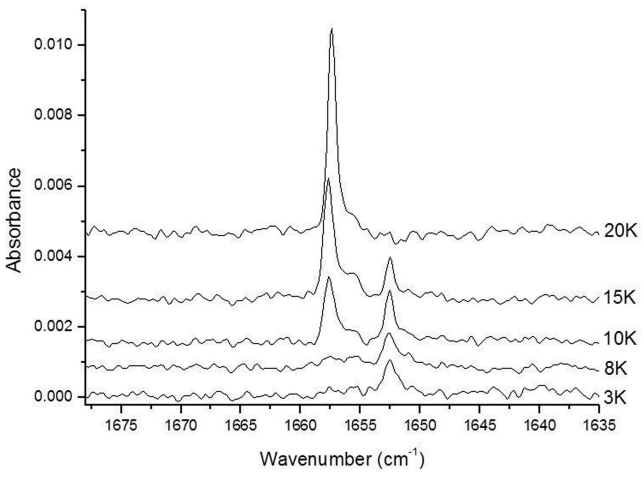

Figure 3. Co-deposition of the N/N_2 mixture at 3 K and successive sample heating between 3 and 20 K.

Consequently, by decreasing the deposition temperature of the sample, we prove that N_3 is formed in the solid phase from the $N + N_2$ reaction. To gain more insight on the $N + N_2$ reaction in the solid phase, the sample formed at 3 K has been gradually heated from 3 to 35 K to control the N-atom mobility and to monitor the yield of N_3 formation. First, the sample was formed and kept at 3 K for 2 h and then probed by recording several IR spectra every 15 min during this period. From the recorded spectra during these 2 h, no change has been noticed, as at temperatures as low as 3 K, all the reactants are completely blocked and accordingly no reaction would take place. Thereafter, the temperature of the sample has been increased at different steps ranged between 3 and 35 K to induce a controlled mobility of N atoms in the sample. Fig. 3 shows the evolution of the two infrared signals characteristic of N_3 trapped in the α and β sites in the nitrogen matrix, when the temperature of the sample is increased in the range of 3–20 K. Between 3 and 10 K the signal at 1652 cm^{-1}, due to N_3 trapped in site α, increases slowly and starts decreasing at 15 K to completely disappear at 20 K. Conversely, the signal at 1657 cm^{-1}, corresponding to N_3 trapped in the site β, is not detected at 3 K. It grows considerably around 10 K and continues to increase, reaching its maximum at 20 K, and then starts to decrease at temperatures higher than 25 K. At temperatures higher than 20 K, the behaviour of the N_3 signal is similar to that shown in Fig. 2.

These results show that by heating the sample gradually between 3 and 20 K, we induce a mobility of N atoms to support the formation of N_3. With this method, the total amount of N_3 formed at each temperature can be deduced from the sum of the integrated peak areas at 1652 and 1657 cm^{-1}. The total and then the highest amount of N_3 formed under our experimental conditions can be deduced from the spectrum of the sample heated at 20 K (Fig. 3).

Fig. 4 shows the formation yield of N_3 and its distribution in the two trapping sites α and β in the nitrogen matrix at different temperatures ranging between 3 and 20 K. At 3 K, only 16 per cent of the total amount of N_3 is produced and trapped exclusively in site α. At 10 K, 72 per cent of the total amount of N_3 is produced, with 35 per cent trapped in site α and 65 per cent in site β. At 15 K, 86 per cent of the total amount of N_3 is produced, with 15 per cent trapped in site α and 85 per cent in site β, while the maximum amount of N_3, trapped totally in site β, is reached at 20 K.

If the two trapping sites α and β were to be correlated to two different structures of solid N_2, the N_3 amount distributions between the α and β sites versus temperature would then inform on the temperatures and structures of the nitrogen matrix. At temperatures lower than 10 K, only one specific structure of solid nitrogen is favoured, corresponding to one definite trapping site for N_3 (structure α, site α) while at temperatures higher than 20 K, the structure β is supported, related to the trapping site β. Finally, at temperatures ranging between 10 and 20 K, the solid nitrogen shows the two mixed structures α and β (Fig. 4).

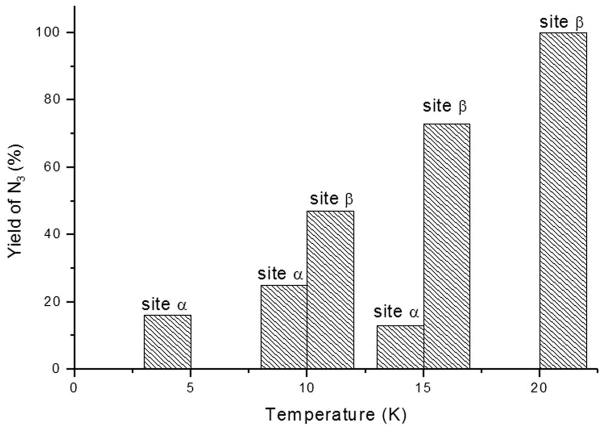

Figure 4. Formation yield of N_3 and its distribution in the two trapping sites α and β in a nitrogen matrix at temperatures ranging between 3 and 20 K.

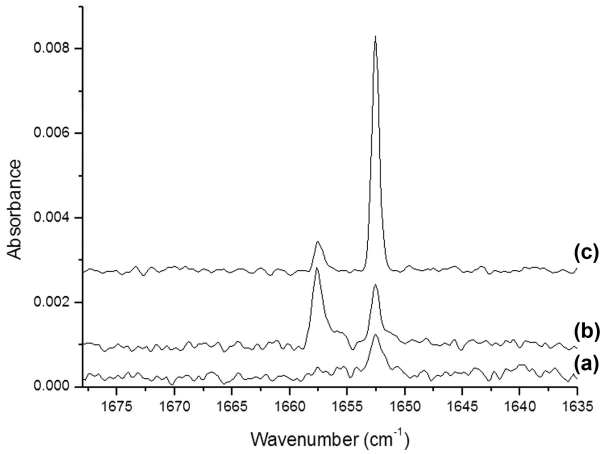

Figure 5. Influence of the deposition temperature on the N + N_2 reaction for the same N/N_2 deposited amount: (a) N/N_2 co-deposition at 3 K; (b) N/N_2 co-deposition at 3 K followed by sample heating at 10 K; (c) N/N_2 co-deposition at 10 K.

To compare the two experimental methods – deposition at 10 K versus deposition at 3 K followed by a sample heating at 10 K – Fig. 5 shows the principal differences for N_3 formation at 10 K. The deposition of the sample at 10 K enhances considerably the yield of N_3 trapped in site α, where 90 per cent of the total amount of N_3 is trapped in site α and only 10 per cent in site β, while for the N/N_2 co-deposition at 3 K followed by a sample heating at 10 K, the amount of N_3 trapped in site β becomes twice as high as that trapped in site α. Thus, we conclude that the relative intensities of these two signals at 1652 and 1657 cm^{-1} might be linked to two structures of the nitrogen ice, which depend strongly on the temperature of the ice growth.

3.3 Monitoring in time the formation of N_3

We choose to follow the kinetic rates of the N + N_2 reaction at 15 K, a temperature at which the mobility of N atoms is more significant than at 10 K and at which the reaction would still take place to form N_3. The N/N_2 sample formed at 3 K has been heated at 15 K and the

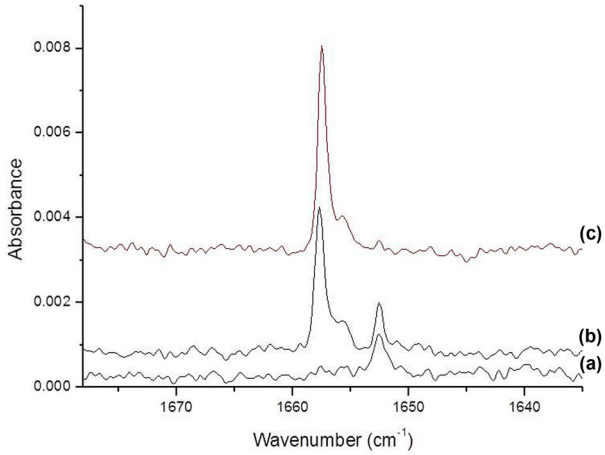

Figure 6. Kinetics of N_3 formation at 15 K: (a) co-deposition of N/N_2 mixture at 3 K; (b) after sample heating at 15 K for 10 min; (c) 3 h later with the sample temperature maintained at 15 K.

kinetics of the N + N_2 reaction has been investigated for more than 3 h, without supplying additional energy to the system. During this period, several IR spectra have been recorded at 15 K to monitor the evolutions of the two N_3 characteristic signals at 1652 and 1657 cm^{-1}. Figs 6(a)–(c) show the IR spectra of an N/N_2 sample formed at 3 K, heated at 15 K for 10 min and and 3 h, respectively. We notice from Fig. 6(c) that the signal at 1652 cm^{-1} corresponding to N_3 trapped in site α vanishes, while that corresponding to N_3 trapped in site β at 1657 cm^{-1} increases. However, there is no clear link between the decreasing signal at 1652 cm^{-1} and the increasing signal at 1657 cm^{-1} and each signal seems to have its own kinetic rate.

Figs 7(a) and (b) show the evolution over time of the integrated peaks at 1652 and 1657 cm^{-1}, respectively, while the sample temperature is maintained at 15 K. We note that at 15 K, in a sample containing N, N_2 and N_3 species, the amount of N_3 trapped in site α decreases over time and it can be fitted with a first-order exponential with a decay constant of 4.5 × 10^{-4} s^{-1} (Fig. 7a), whereas the amount of N_3 trapped in site β increases and can be fitted with a first-order exponential growth with a rate constant of 7 × 10^{-4} s^{-1} (Fig. 7b).

As the amount of N_3 trapped in site β increases almost twice as fast as the amount of N_3 trapped in site α decreases, the total amount of N_3 formed in the nitrogen matrix increases over time (Fig. 7c) and it can be fitted with a second-order exponential growth with two characteristic constants of 3.5 × 10^{-4} s^{-1} and 2.2 × 10^{-3} s^{-1}. Those kinetic rates are discussed in Section 4.

3.4 UV-visible photo-irradiation of N_3

As shown previously, the total and then the highest amount of N_3 formed in the solid phase, under our experimental conditions, are reached when the sample is heated at 20 K, a temperature at which N_3 is exclusively trapped in site β, whatever the deposition temperature. We have investigated the behaviour of N_3 exposed to different selective UV-visible radiations using a Xe–Hg lamp coupled to different filters and we have found that N_3 is dissociated only at wavelengths lower than 280 nm. Fig. 8 shows the results obtained for a sample irradiated at 280 and 265 nm, where N_3 decomposes efficiently at 265 nm. The kinetics of N_3 photodecomposition at

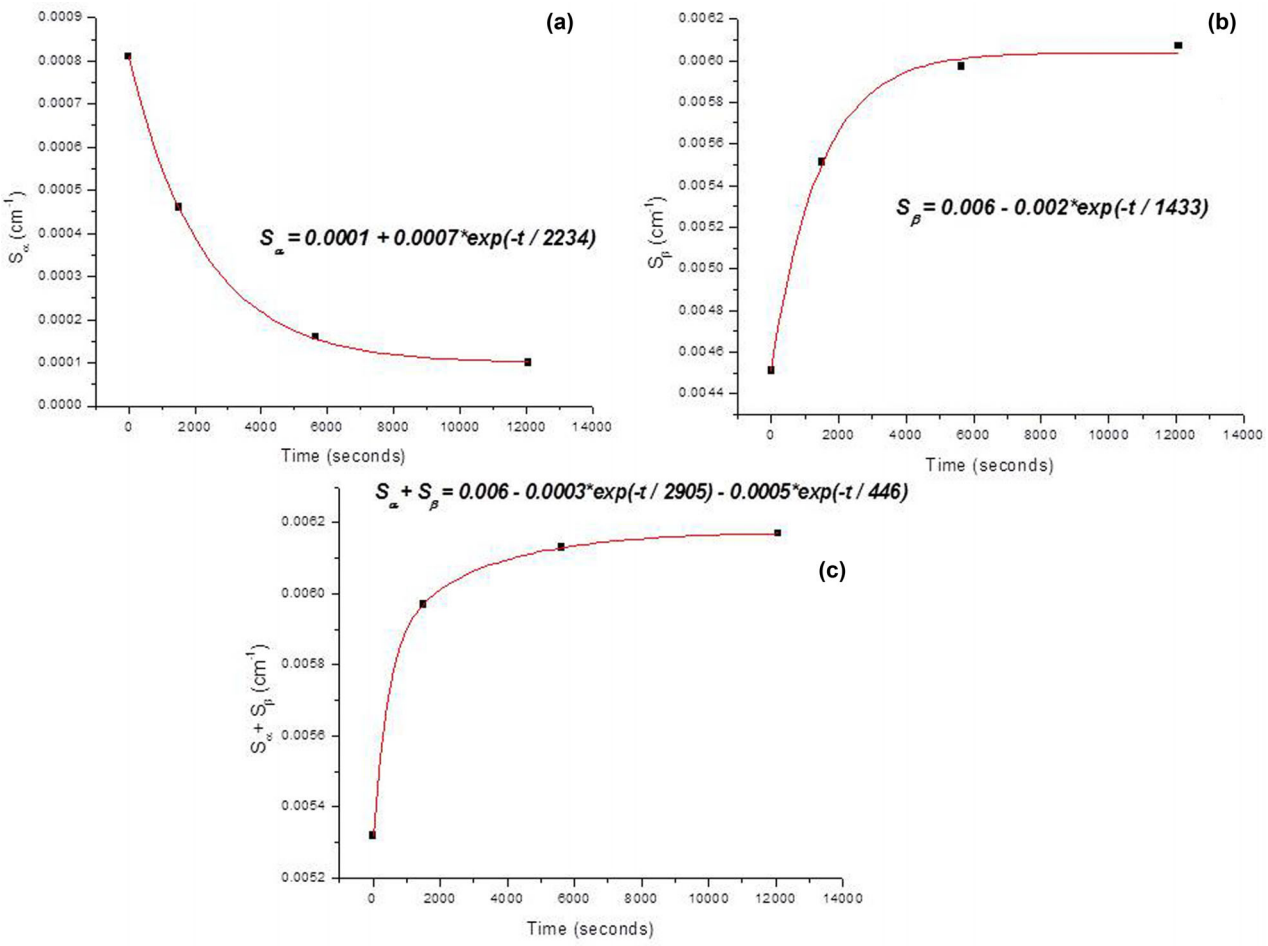

Figure 7. Behaviour over time of the amount of N_3 trapped: (a) in site α; (b) in site β; (c) in a nitrogen matrix (α and β sites).

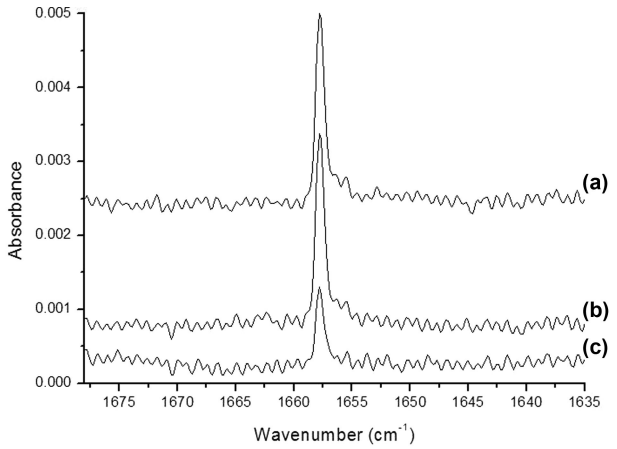

Figure 8. Behaviour of N_3 exposed to two selected UV radiations: (a) co-deposition of N/N_2 mixture at 3 K followed by sample heating at 20 K to reach the maximum amount of N_3; (b) sample irradiation at 280 nm; (c) sample irradiation at 265 nm.

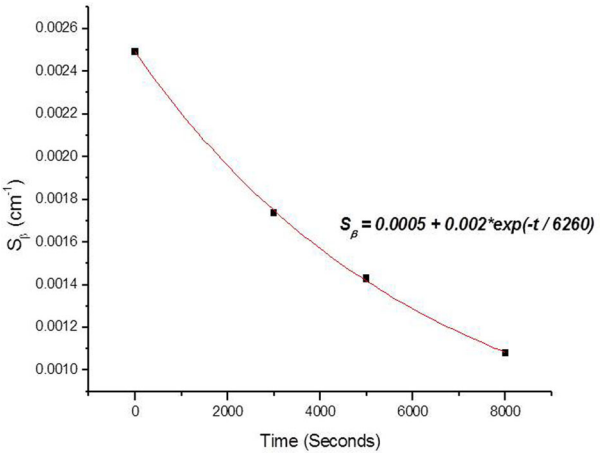

Figure 9. Behaviour over time of N_3 photodecomposition at 265 nm.

265 nm has been studied over time and it follows a first-order model with respect to the concentration of N_3 trapped in solid nitrogen (Fig. 9), with a photolysis constant estimated to be around 1.6×10^{-4} s^{-1}.

4 DISCUSSION

In the following, we discuss all the possible explanations for the formation of N_3 in the solid phase. From the experiments carried out at 3 K, we have shown that N_3 is formed in the solid phase, by inducing the mobility of N atoms trapped in the nitrogen matrix. We summarize in Table 4 some thermodynamic data of reactions that are important for the present study.

Table 4. Thermodynamic data of reactions: activation and formation energies.

Reaction	*Ea*/(kJ mol^{-1})	ΔH/(kJ mol^{-1})	References and comments
N(^{2}S)		470.5[a]	Frost & McDowell (1956)
N(^{2}D)		701.5[b]	Jamieson & Kaiser (2007)
N(^{2}P)		815.5[c]	Sansonetti & Martin (2005)
N_2(A)		600	Kadochnikov et al. (2013)
N_2(X)		0	By definition
N(^{4}S) + N_2(X) → N_3(X)	219	0.960	Zhang et al. (2005)
N(^{4}S) + N_2 → N_3(X)		–14.5[d]	Deduced
N(^{2}D) + N_2(X) →N_3(X)	13.2	–236	Zhang et al. (2005)
3/2 N_2 → N_3(X)		456	Dixon et al. (2004)
N(^{4}S) + N(^{4}S) → N_2(X)		–941	Frost & McDowell (1956)
N(^{4}S) + N(^{4}S) → N_2(A)		–341	Kadochnikov et al. (2013)
N_2(A) → N_2(X)		–600	Kadochnikov et al. (2013)
N(^{2}D) → N(^{4}S)		–231[e]	Deduced

[a]The value reported by Frost & McDowell divided by 2.
[b]Deduced from the text of Jamieson & Kaiser.
[c]Calculated from the spectral lines reported in the *Handbook of Basic Atomic Spectroscopic Data* of the National Institute of Standards and Technology (Sansonetti & Martin 2005).
[d]Calculated by us using the data of Dixon et al. (2004) and Frost & McDowell (1956).
[e]Calculated by us using the data of Jamieson & Kaiser (2007) and Frost & McDowell (1956).

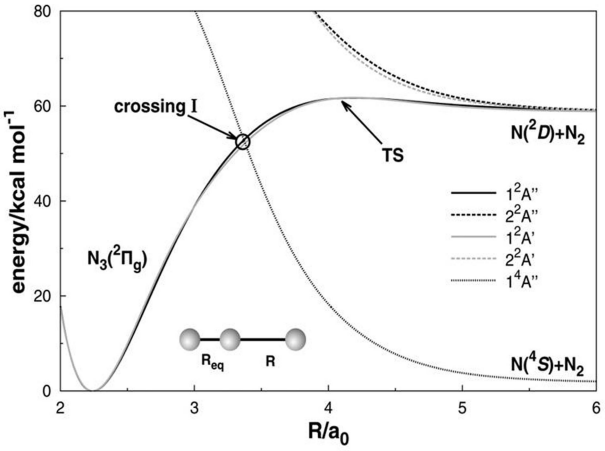

Figure 10. Energy diagram of the N + N_2(X) → N_3 reaction taken from Galvão et al. (2013).

4.1 Formation of N_3: chemical pathways, kinetic rates and energies

4.1.1 N(^{4}S) + N_2(X) → N_3 one-step reaction mechanism, involving one nitrogen atom

The reaction N(^{4}S) + N_2(X) → N_3 associated with interactions between N(^{4}S) and N_2(X) in one step could not take place as we have already revealed that the N/N_2 sample formed and kept for 2 h at 3 K showed no evolution and thus no N_3 formation.

In fact, as the N/N_2 solid sample is a result of a co-deposition of atomic and molecular nitrogen derived from a plasma discharge, the only possibility to attest that all the trapped species are really the ground state, and that N(^{4}S) + N_2(X) would be the only potential reaction, is to keep the N/N_2 solid sample at 3 K over a period of time in order to allow a complete relaxation of the studied system. Additionally, according to energy diagrams available in the literature (Fig. 10), such a reaction occurring in one step and involving N and N_2 in their ground states exhibits very high activation energies of the order of 220–250 kJ mol^{-1} (Zhang, Morokuma & Wodtke 2005; Galvão et al. 2013). However, the reaction involving excited N atoms N(^{2}D) + N_2 → N_3 is highly exothermic ($\Delta H = -240$ kJ mol^{-1}) with a tiny energy barrier around 13 kJ mol^{-1} and it seems to be more favourable.

Regarding the energy diagram given in Fig. 10, the formation of the N_3 radical from the N(^{4}S) + N_2(X) reaction should be possible only by providing energies of the order of 250 kJ mol^{-1} to the system. As we do not provide additional energy to the system, the N(^{4}S) + N_2(X) → N_3 reaction would occur by involving more than one step.

4.1.2 N(^{4}S) + N_2(X) → N_3 two-step reaction mechanism, involving two nitrogen atoms

The formation of some energetic intermediates could contribute to providing the required energy to form the N_3 radical from the N(^{4}S) + N_2(X) reaction. First, the N(^{4}S)-N(^{4}S) recombination reaction, which is exothermic by 341 kJ mol^{-1}, would be possible under our experimental conditions by heating a N/N_2 sample formed at 3 K in the range of 3–20 K, leading to energetic molecular nitrogen N_2(A), which retains an energy of 600 kJ mol^{-1} (Kadochnikov, Loukhovitski & Starik 2013):

$$\mathrm{N}\left(^4\mathrm{S}\right) + \mathrm{N}\left(^4\mathrm{S}\right) \rightarrow \mathrm{N_2\,(A)} \quad \Delta H = -341\,\mathrm{kJmol^{-1}}. \tag{4}$$

Then, the energetic molecular nitrogen N_2(A) may reaction with ground-state molecular nitrogen, forming the solid–N_2 to form N_3 and one nitrogen atom:

$$\mathrm{N_2\,(A) + N_2\,(X) \rightarrow N_3 + N}\left(^4\mathrm{S}\right) \quad \Delta H = +326.5\,\mathrm{kJmol^{-1}}. \tag{5}$$

However, such a process is unfeasible as it is endothermic and it goes against the entropy of the system where two molecules react spontaneously to form two radical species.

4.1.3 N(^{4}S) → N_3 two-step reaction mechanism, involving three nitrogen atoms

Just after the N(^{4}S)–N(^{4}S) recombination reaction to form N_2 (A), ground-state nitrogen atoms may react with N_2 (A) to form the N_3

radical:

$$\mathrm{N}\left(^4\mathrm{S}\right) + \mathrm{N}\left(^4\mathrm{S}\right) \rightarrow \mathrm{N}_2\,(\mathrm{A}) \quad \Delta H = -341\,\mathrm{kJmol}^{-1};$$
$$\mathrm{N}_2\,(\mathrm{A}) + \mathrm{N}\left(^4\mathrm{S}\right) \rightarrow \mathrm{N}_3 \quad \Delta H = -614.5\,\mathrm{kJmol}^{-1}. \tag{6}$$

The reaction pathway (6) is energetically efficient and, even if there are no theoretical models in the literature to characterize it, such a process could not be considered as a pathway of N_3 formation. In fact, the energy released from reaction (6) is almost three times higher than the N_3 binding energy and it might be a source of the N_3 dissociation into the $N(^2D)$ excited atom and N_2 molecule, as shown in Fig. 10:

$$\mathrm{N}_2\,(\mathrm{A}) + \mathrm{N}\left(^4\mathrm{S}\right) \rightarrow (\mathrm{N}_3) \rightarrow \mathrm{N}_2\,(\mathrm{X}) + \mathrm{N}\left(^2\mathrm{D}\right)$$
$$\Delta H = -369\,\mathrm{kJmol}^{-1}. \tag{7}$$

The formation of $N_2(A)$ and $N(^2D)$ excited species from ground-state nitrogen atoms has already been characterized experimentally (Oehler, Smith & Dressler 1977; Savchenko et al. 2015), where the heating between 5 and 20 K of solid nitrogen containing N atoms shows increases of emissions at 300 and 523 nm corresponding to N_2 (A) $\rightarrow$ N_2(X) and $N(^2D) \rightarrow N(^4S)$ molecular and atomic transitions. Those emissions are a result of the thermal induced recombination $N(^4S)$–$N(^4S)$ to form N_2 (A) and to an energy transfer from N_2 (A) to $N(^4S)$ to from $N(^2D)$. In such a situation, $N(^2D)$ should be an intermediate into the N_3 formation reaction.

4.1.4 $N(^4S) \rightarrow N_3$ three-step reaction mechanism, involving three nitrogen atoms

Then, in addition to reactions (4) and (7), N_3 should be formed through reaction (8), which is exothermic, showing very low activation around 13 kJ mol^{-1}. It might be the important pathway for the formation of the N_3 radical:

$$\mathrm{N}\left(^2\mathrm{D}\right) + \mathrm{N}_2\,(\mathrm{X}) \rightarrow \mathrm{N}_3 \quad \Delta H = -245.5\,\mathrm{kJmol}^{-1}. \tag{8}$$

By applying the steady-state approximation, we can easily deduce that the N_3 formation follows a second-order kinetics with respect to the concentration of N_3 as shown:

$$\mathrm{d}\,[N_3]\,/\mathrm{d}t = k_1\,([n_0] - 3\,[N_3])^2. \tag{9}$$

Here, n_0 and $[n_0]$ are the initial amount of atomic nitrogen and the initial concentration of N atoms in the sample, respectively, $[N_3]$ is the concentration of N_3 formed by reaction 8 and k_1 is the rate constant of the $N(^4S)$–$N(^4S)$ recombination reaction. By coupling reactions (4), (7) and (8), we can deduce the concentrations of $N(^4S)$ and N_3 versus time as

$$\frac{1}{[n_0]} - \frac{1}{\left[N\left(^4\mathrm{S}\right)\right]} = 3k_1 t, \tag{10}$$

$$\frac{1}{[N_3]_\infty - [N_3]} - \frac{1}{[N_3]_\infty} = 9k_1 t, \tag{11}$$

where $[N_3]_\infty$ is the final concentration of N_3 at infinite time.

The rate of formation of N_3 in solid nitrogen depends only on k_1, the rate constant of the $N(^4S)$–$N(^4S)$ recombination reaction. It can be deduced experimentally from the total integrated peak area $S = S_\alpha + S_\beta$ from Fig. 7(c) by using the corresponding absorption coefficient ε of the ν_3 vibrational mode of N_3 and the solid sample depth e. We can then show that $\frac{1}{S_\infty - S(t)} - \frac{1}{S_\infty}$ has a linear regression of time with $(9/e\varepsilon)\,k\_1$ as the slope (Fig. 11):

$$\frac{1}{S_\infty - S(t)} - \frac{1}{S_\infty} = \frac{9}{e\varepsilon}\,k_1 t. \tag{12}$$

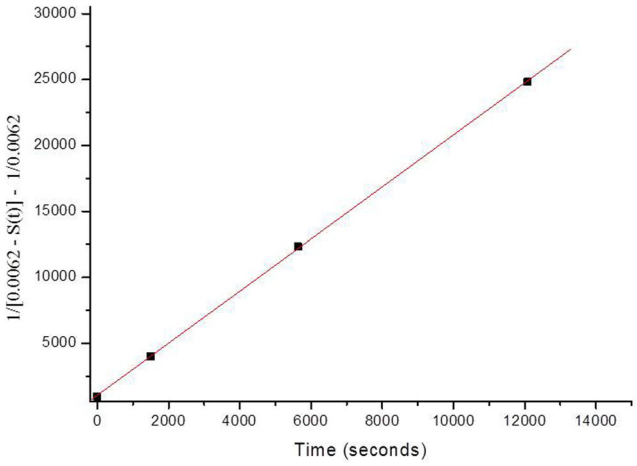

Figure 11. Behaviour over time of the total amount of N_3 trapped in the nitrogen matrix, $\{1/[S_\infty - S(t)]\} - (1/S_\infty)$. Data are deduced from the total integrated peak area $S = S_\alpha + S_\beta$ from Fig. 7(c).

From Fig. 11, we show that the total amount of N_3 depends strongly on k_1. However, the kinetics of N_3 formation in solid nitrogen could be more complex if we have to distinguish between the N_3 trapped in site α and that in site β. In fact, in addition to the $N(^4S)$–$N(^4S)$ recombination processes and $N_2(A) + N(^4S) \rightarrow N_2$ (X) + $N(^2D)$ energy transfer mechanisms, the formation of N_3 in two trapping sites, the migration of N_3 from site α to site β, could be taken into account but they globally do not influence the evolution of the total amount of N_3 as shown:

$$\mathrm{N}\left(^4\mathrm{S}\right) + \mathrm{N}\left(^4\mathrm{S}\right) \rightarrow \mathrm{N}_2\,(\mathrm{A})$$

$$\mathrm{N}_2\,(\mathrm{A}) + \mathrm{N}\left(^4\mathrm{S}\right) \rightarrow \mathrm{N}_2\,(\mathrm{X}) + \mathrm{N}\left(^2\mathrm{D}\right)$$

$$\mathrm{N}\left(^2\mathrm{D}\right) + \mathrm{N}_2\,(\mathrm{X}) \rightarrow \mathrm{N}_3(\alpha) \tag{13}$$

$$\mathrm{N}_3(\mathrm{a}) \rightarrow \mathrm{N}_3(\beta) \tag{14}$$

$$\mathrm{N}\left(^2\mathrm{D}\right) + \mathrm{N}_2\,(\mathrm{X}) \rightarrow \mathrm{N}_3(\beta). \tag{15}$$

From these equations, we deduce the amounts of $N(^4S)$, $N_3(\alpha)$ and $N_3(\beta)$ versus time:

$$\frac{1}{[n_0]} - \frac{1}{\left[N\left(^4\mathrm{S}\right)\right]} = 3k_a t \tag{16}$$

$$[N_3\,(\alpha)] = K e^{-k_d t} \tag{17}$$

$$[N_3\,(\beta)] = [n_0] - K e^{-k_d t} - \frac{2}{\left(\frac{1}{[n_0]} - 3k_a\right)^2}. \tag{18}$$

Here, k_a and k_d – i.e. the appearance of $N_2(A)$ and the disappearance of $N_3(\alpha)$ – are the rate constants of reactions (4) and (14), n_0 is the initial amount of $N(^4S)$ and K is a time-dependent function. From these kinetic studies, we can deduce the rate constants of reactions and also the absorption coefficient of N_3.

4.2 Determination absorption coefficient of N_3

From experiments carried out at 3 and 10 K, we have shown that the total amount of N_3 formed in solid nitrogen is trapped exclusively

in site β when the sample is heated at 20 K, whatever the deposition temperature. Thus, we can estimate the amount of N_3 in our samples as

$$n_{N_3} = n\, s, \tag{19}$$

where n is the column density of N_3 and s is the surface of the sample ($s = 1$ cm^2 in the present work).

Under our experimental conditions, we define the column density as

$$n = \frac{\ln 10 \int I(\upsilon)}{\varepsilon} \frac{\cos(8^\circ)}{2}, \tag{20}$$

where $\int I(\upsilon) = S_\beta$ (cm^{-1}) is the integrated peak area at 1657 cm^{-1} of N_3 trapped in site β and measured at 20 K. The cos(8°)/2 is a correction term that takes into account the geometry of our IR measurements (Bennett et al. 2004). If we suppose that all the nitrogen atoms are converted in the solid phase into the azide radical (3 N → N_3), the upper limit of the total amount of N_3 trapped in solid nitrogen can be estimated to be one-third of the initial quantity of N atoms n_0 stemming from the microwave discharge and reaching the solid sample:

$$n_{N_3} = \frac{n_0}{3} = 1.14\, \frac{S_\beta}{\varepsilon} s. \tag{21}$$

We deduce the absorption coefficient of N_3 as

$$\varepsilon = 3.42\, \frac{S_\beta}{n_0} s. \tag{22}$$

Under our experimental conditions, we can estimate n_0 to be around 4.8×10^{17} atoms and the absorption coefficient ε of N_3 to be around 4.5×10^{-20} cm molecule^{-1}, which is closer to the value given by Moore et al. ($\varepsilon = 7.2 \times 10^{-20}$ cm molecule^{-1}) than to that calculated by Jamieson & Kaiser (2007), i.e. $\varepsilon = 4 \times 10^{-17}$ cm molecule^{-1}.

4.3 Determination of the rate constant of $N(^4S) + N_2 \rightarrow N_3$ reaction in the solid phase

We have shown that the rate of formation of N_3 in solid nitrogen depends only on k_1, the rate constant of the $N(^4S)$–$N(^4S)$ recombination reaction. By studying the behaviour against time of the total amount of N_3 trapped in the nitrogen matrix, we have shown that $\frac{1}{S_\infty - S(t)} - \frac{1}{S_\infty}$ is a linear function of time with a slope $(9/e\varepsilon)$ $k_1 = 1.97$ (Fig. 11). Knowing the sample depth e and the absorption coefficient ε of N_3, we can deduce the rate constant k_1 of the $N(^4S)$–$N(^4S)$ recombination reaction and also that of the N_3 formation $9k_1$. Bernstein and Sandford (1999) gave the value of N_2 vibration absorption coefficient ε_{N2} at 1.8×10^{-22} cm molecule^{-1}. The thickness e of a solid nitrogen can be defined by

$$e = \frac{n_{N_2}}{\rho_{N_2}}, \tag{23}$$

where n_{N_2} and ρ_{N_2} (1.0271 g cm^{-3}) are the column density and the density of N_2, respectively (Bernstein & Sandford 1999). The n_{N_2} column density can be estimated from the integrated peak area of N_2 vibration at 2328 cm^{-1} ($S_{N_2} = 0.003$ cm^{-1} measured from our spectra recorded at 3 K):

$$n_{N_2} = 1.14\, \frac{S_{N_2}}{\varepsilon_{N_2}}. \tag{24}$$

Under our experimental conditions, we found the thickness of the sample e to be around 8.6 μm and the rate constant k_1 of the $N(^4S)$–$N(^4S)$ recombination reaction to be about 8.5×10^{-24} s^{-1} molecule^{-1} cm^3 and that for N_3 formation to be 7.7×10^{-23} s^{-1} molecule^{-1} cm^3.

Slanger & Black (1976) measured the rate constant for the quenching reaction $N(^2D) + N_2(X) \rightarrow N(^4S) + N_2(X)$ in the gas phase over the temperature range of 198–372 K. They reported the quenching rate expression as $k_T = 10^{-13} \exp(-513/T)$ s^{-1} molecule^{-1} cm^3, which at 24 K would be $k_{24\,K} = 5.2 \times 10^{-23}$ s^{-1} molecule^{-1} cm^3. This quenching rate calculated at 24 K is the same order of magnitude as the rate constant we measured for the formation of N_3. In fact, the highest amount of N_3 formed under our experimental conditions is reached when the sample is heated between 20 and 25 K.

4.4 N_3 containing N_2 ices in space

In addition to the formation of N_3 in the solid phase, we show that N_3 decomposes efficiently when exposed to soft UV light ($280 < \lambda < 220$ nm), which is not energetic enough to dissociate molecular nitrogen. This might explain why Hudson & Moore (2002) did not detect N_3 by irradiating N_2 ices using a 121-nm hydrogen discharge lamp while Wu et al. (2012) have shown that the UV photolysis of a solid nitrogen with a tunable UV light at 121 nm leads necessarily to N_3 radical formation. Hudson & Moore justified the non-detection of N_3 by the fact that the UV energy at 121 nm was not strong enough to fragment the molecular nitrogen into atomic nitrogen, while Wu et al. detected N_3 using similar photon fluxes and UV wavelength with a slight variation. This could be the source of the difference between the two experimental methods and might be linked to the photodecomposition of N_3 that we have studied using soft UV photons.

The variation is that Hudson & Moore used a broad-band hydrogen UV lamp, which delivers photons at 121 nm and also rays at higher wavelengths, while Wu et al. used a monochromatic photolysis at 121 nm to form N_3. The non-detection of N_3 by Hudson & Moore is then a result of the N_3 photodecomposition, due to the soft UV light from the broad-band hydrogen lamp, which seems more efficient than its formation through the N_2 + 121 nm photoreaction, and this may be one of the reasons why it is not yet detected in the interstellar medium. Also, the non-delectability of N_3 and its derivatives such as HN_3 or N_3^- would be because all those chemical species react efficiently with ions, radicals and even stable molecules, and would be a source of many chemical transformations in space. They are already used as oxidants in fast kinetic studies (Alfassi et al. 1987), playing an important role in the atmospheric photochemistry (Orlando et al. 2005) of hydrazoic acid (HN_3).

However, we have shown that for the formation of N_3 containing N_2 ices at 10 K, 90 per cent of the total amount of N_3 is trapped in site α, absorbing at 1652 cm^{-1}, while for similar experiments carried out at 3 K followed by heating at 10 K, the amount of N_3 trapped in site β (at 1657 cm^{-1}) is twice as high as that trapped in site α. At temperatures higher than 15 K, or when N_3 is formed using high-energy sources (particle or photon bombardments), N_3 absorbs mainly at 1657 cm^{-1}. Subsequently, the relative intensities of these two signals at 1652 and 1657 cm^{-1} to quantify the azide radical, if measurable in the future from space observations, would inform on the structures of nitrogen ices in molecular clouds and on the environment of the growth of N_2 ices in the interstellar medium or in regions where temperatures are low enough to form solid nitrogen.

5 CONCLUSION

We provide a final clarification for the formation mechanism of N_3 in the solid phase when the reactants N and N_2 are mixed in the gas phase and co-deposited on a surface maintained at temperatures in the range of 3–10 K. We have shown that the signals at 1652 and 1657 cm^{-1} used to characterize N_3 spectroscopically are directly linked to the method of generating the azide radical and also to the temperature of its formation. Therefore, the relative intensities of these two signals at 1652 and 1657 cm^{-1}, if measurable in the future from space observations, would inform on the structures of nitrogen ices and their environments in molecular clouds or in regions where temperatures are low enough to form N_2 ices. To specify the presence of N_3 in the solid phase, the signal at 1657 cm^{-1} is supported when N_3 is formed using photon irradiation or energetic particle bombardments regardless of formation temperatures. However, when N_3 is produced by co-condensing non-energetic N atoms and molecular N_2, the signal at 1652 cm^{-1} is favoured for temperatures lower than 15 K and that at 1657 cm^{-1} at higher temperatures. We show through this study that the rate of formation of N_3 in solid nitrogen follows a second-order kinetics with respect to the concentration of N_3 and depends only on k_1, the rate constant of the $N(^4S)-N(^4S)$ recombination reaction. A rate constant of 7.7×10^{-23} s^{-1} $molecule^{-1}$ cm^3 has been measured for N_3 formation in the solid phase at 15 K. Finally, we explain that the non-detection of N_3 in space might be a result of the N_3 photodecomposition under exposition to soft UV light, which is not energetic enough to dissociate molecular nitrogen but is efficient enough to decompose N_3.

ACKNOWLEDGEMENTS

This work was supported in part by the LabEx MiChem, French state funds managed by the French National Research Agency (ANR) within the Investissements d'Avenir programme under reference ANR-11-IDEX-0004-02.

REFERENCES

Alfassi Z. B., Harriman A., Huie R. E., Mosseri S., Neta P., 1987, J. Phys. Chem., 91, 2120
Amicangelo J. C., Collier J. R., Dine C. T., Saxton N. L., Schleicher R. M., 2007, Mol. Phys., 105, 989
Bennett C. J., Jamieson C., Mebel A. M., Kaiser R. I., 2004, PCCP, 6, 735
Bernstein M. P., Sandford S. A., 1999, Spectrochim. Acta. Mol. Biomol. Spectrosc., 55, 2455
Dixon D. A. et al., 2004, J. Am. Chem. Soc., 126, 834
Frost D. C., McDowell C. A., 1956, Proc. R. Soc. London A,236, 278
Galvão B. R. L., Varandas A. J. C., Braga J. P., Belchior J. C., 2013, J. Phys. Chem. Lett., 4, 2292
Gerakines P. A., Schutte W. A., Ehrenfreund P., 1996, A&A, 312, 289
Hudson R. L., Moore M. H., 2002, ApJ, 568, 1095
Jamieson C. S., Kaiser R. I., 2007, Chem. Phys. Lett., 440, 98
Kadochnikov I. N., Loukhovitski B. I., Starik A. M., 2013, Plasma Sources Sci. Technol., 22, 1
Khabasheku V. N., Margrave J. L., Waters K., Schultz J. A., 1997, J. Appl. Phys., 82, 1921
Maret S., Bergin E. A., Lada C. J., 2006, Nature, 442, 427
Milligan D. E., Brown H. W., Pimentel G. C., 1956, J. Chem. Phys., 25, 1080
Oehler O., Smith D. A., Dressler K., 1977, J. Chem. Phys., 66, 2097
Orlando J. J., Tyndall G. S., Betterton E. A., Lowry J., Stegall S. T., 2005, Environ. Sci. Technol., 39, 1632
Sansonetti J. E., Martin W. C., 2005, J. Phys. Chem., 34, 4
Savchenko E. V., Khyzhniy I. V., Uyutnov S. A., Barabashov A. P., Gumenchuk G. B., Beyer M. K., Ponomaryov A. N., Bondybey V. E., 2015, J. Phys. Chem. A, 119, 2475
Slanger T. G., Black G., 1976, J. Chem. Phys., 64, 4442
Tian R., Facelli J. C., Michl J., 1988, J. Phys. Chem., 92, 4073
Wu Y-J., Wu C. Y. R., Chou S-L., Lin M-Y., Lu H-C., Lo J-I., Cheng B-M., 2012, ApJ, 746, 175
Zhang P., Morokuma K., Wodtke A. M., 2005, J. Chem. Phys., 122, 14106
Zins E. L., Joshi P. R., Krim L., 2011, MNRAS, 415, 3107

This paper has been typeset from a Microsoft Word file prepared by the author.